Supporting Information

Kwiatkowski et al. 10.1073/pnas.1007349107

SI Text

SI Materials and Methods. ***Protein expression vectors.*** Hmp-1, HMP-2, and HMR-1^{cyt} cDNAs were cloned in a pGEX-TEV vector, a modified pGEX-KG vector into which a tobacco etch virus (TEV) site was inserted to permit cleavage of the N-terminal GST tag with TEV protease. Fragments of Hmp-1—aa 1–676, aa 677–904 and aa 677–927—were generated by PCR amplification using pGEX-TEV-Hmp-1 as a template and cloned into pGEX-TEV. The N-terminal 35 amino acid deletion mutant of HMP-2 (HMP-2ΔN) was subcloned into pGEX-TEV plasmid in a similar manner. All constructs were verified by sequencing. Full-length chicken vinculin in pET15b was kindly provided by Dr. R. Liddington.

GST pull-downs. 5 μg of GST-HMP-2 bound to glutathione agarose beads was incubated with 1 to 25 μg of HMP-1 in 500 μL of Elution Buffer (20 mM Tris pH 8.0, 150 mM NaCl, 2 mM EDTA, 10% glycerol and 1 mM DTT). Samples were rotated for 1 h at room temperature, washed three times with 1.0 mL of PBSTR (1X PBS, 0.05% Tween 20 and 5 mM DTT) and 40 μL of 1X Laemmli sample buffer was added to the bead bed. 20 μL of all samples were separated by SDS-PAGE on a 4–15% gradient gel. Gels were stained with Coomassie blue, destained and then imaged on a LI-COR scanner. For quantification, gel band intensities were measured in ImageJ, normalized, and plotted.

SAXS analysis. Small angle scattering data were collected at beamline 4.2 at the Stanford Synchroton Radiation Laboratory (SSRL). Data were recorded at a wavelength of 1.13 or 1.38 Å with 10 exposures. All proteins were prepared in 20 mM Tris pH 8.0, 150 mM Na acetate pH 8.0 and 1 mM DTT. For each protein, data were measured at different concentrations from 4.5–35 mg/ml). A buffer blank was measured before each sample and subtracted to remove the bulk solvent contribution. Data from different concentrations were scaled and merged for subsequent analysis. The radius of gyration R_g was computed using the program Primus (1). Data used for Guinier plot analysis was restricted to scattering angles for which the product $q \times (\text{estimated } R_g) \leq 1.3$, assuming a spherical molecule of uniform density for estimating R_g. All datasets were truncated at $q = 0.3$, the resolution of the lowest resolution dataset, for calculation of the maximum distance vector D_{max} and the pair distribution function $P(r)$ in the program GNOM (2). The pair distribution function $P(r)$ was calculated for different D_{max} values, and the D_{max} values in Table 1 were chosen according to two criteria: (*i*) that the $P(r)$ distribution approach zero smoothly, and (*ii*) that the R_g computed by transformation of the $P(r)$ for a given D_{max} agreed with the R_g obtained from the Guinier analysis. The range in which D_{max} could vary and meet these criteria was used as an estimate of its error, provided in Table 1.

Yeast two-hybrid analysis. DNA inserts for FL HMP-2 (aa 1–678), FL HMP-1 (aa 1–927), HMP-1 aa 1–676 (head domain), and HMP-1 aa 677–927 (tail domain) were generated by PCR and cloned into pGBT9, to generate GAL4 DNA-binding domain fusions, and pACT2, to generate GAL4 activation domain fusions. All constructs were confirmed by sequencing. Fusion constructs in pGBT9 were transformed into PJ69-4A (*MAT*a, *trp1-901*, *leu2-3, 112, ura3-52, his3-200, gal4Δ, gal80Δ, LYS2*::*GAL1p-HIS3, GAL2p-ADE2, MET2*::*GAL7p-lacZ*) and pACT2 constructs were transformed into PJ69-4α (*MAT*α, *trp1-901, leu2-3, 112, ura3-52, his3-200, gal4Δ, gal80Δ, LYS2*::*GAL1p-HIS3, GAL2p-ADE2*) (3). The resulting strains were mated to generate all possible pairwise combinations and diploids selected on medium lacking leucine and tryptophan. Diploids were grown to saturation in selective medium, plated in serial dilutions on medium lacking histidine and adenine to monitor *GAL* promoter activation, and grown at 30 °C for the time indicated.

DIC and fluorescent imaging. Transgenic embryos were isolated from gravid hermaphrodites, mounted on an agarose slide and aged at 20–25 °C until the onset of morphogenesis. For DIC images, a Nikon Optiphot-2 confocal microscope with Dage/MTI camera, Scion framegrabber, and Macintosh G4 computer running Image J (http://rsbweb.nih.gov/ij/) using custom macros/plugins (available at http://worms.zoology.wisc.edu/research/4d/4d.html) was used to collect images with a 60x/1.40 oil objective at 20 °C. For fluorescent imaging, a Perkin–Elmer UltraVIEW spinning disk confocal microscope attached to a Nikon Eclipse E600 microscope and Hamamatsu ORCA-ER camera was used to collect images of EGFP-expressing embryos at 3 min intervals with a 60x/1.40 oil objective at 20 °C, or of antibody and phalloidin staining with a 100x/1.45 oil objective. EGFP expression levels were determined by measuring the total fluorescent intensity of individual mutant embryos. HMP-1::EGFP ($n = 6$) and HMP-1::EGFP(Δ13–185) ($n = 7$) were expressed at comparable levels (6806 versus 6835, arbitrary units). To improve image acuteness, an unsharp mask filter was applied equally to related images in Adobe Photoshop.

1. Konarev PV, Volkov VV, Sokolova AV, Koch MHJ, Svergun DI (2003) PRIMUS: A Windows PC-based system for small-angle scattering data analysis. *J Appl Crystallogr* 36(5):1277–1282.
2. Svergun D (1992) Determination of the regularization parameter in indirect-transform methods using perceptual criteria. *J Appl Crystallogr* 25(4): 495–503.
3. James P, Halladay J, Craig EA (1996) Genomic libraries and a host strain designed for highly efficient two-hybrid selection in yeast. *Genetics* 144(4): 1425–1436.

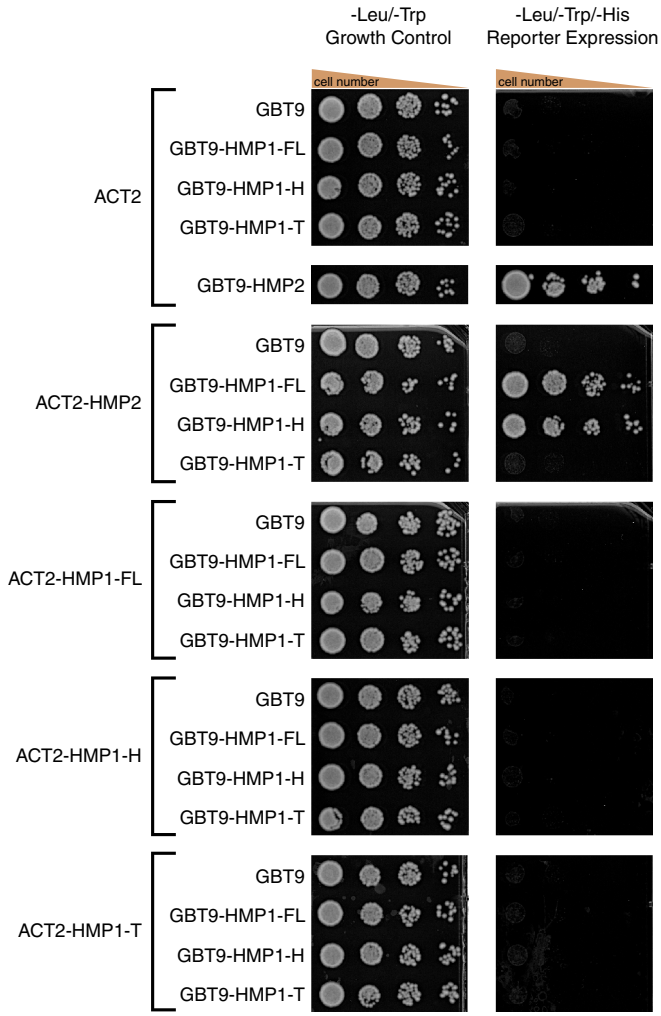

Fig. S1. Yeast two-hybrid analysis of HMP-1 and HMP-2 interactions. HMP-1 FL protein, HMP-1 aa 1–676 (head domain, H), HMP-1 aa 677–927 (tail domain, T) and HMP-2 FL protein were cloned into pGBT9 (fusion to GAL4 DNA-binding domain) and pACT2 (fusion to GAL4 activation domain). Individual constructs were transformed into yeast, and diploid combinations spotted as a dilution series onto -Leu/-Trp media to test for growth and -Leu/-Trp/-His media to measure reporter expression. Growth after two days shown. When fused to the DNA-binding domain of GAL4, HMP-2 initiated transcription in the absence of any activator (auto-activation); the HMP-2-GAL4 activation domain did not auto-activate and was used for all interaction studies. HMP-2 interacted strongly with HMP-1 FL and HMP-1 H but not with HMP-1 T. No other interactions were detected.

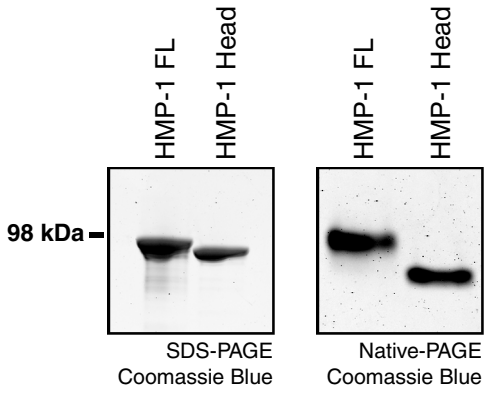

Fig. S2. Recombinant FL HMP-1 and HMP-1 aa 1–676 (head domain) were separated by SDS-PAGE (*Left*) or native-PAGE (*Right*).

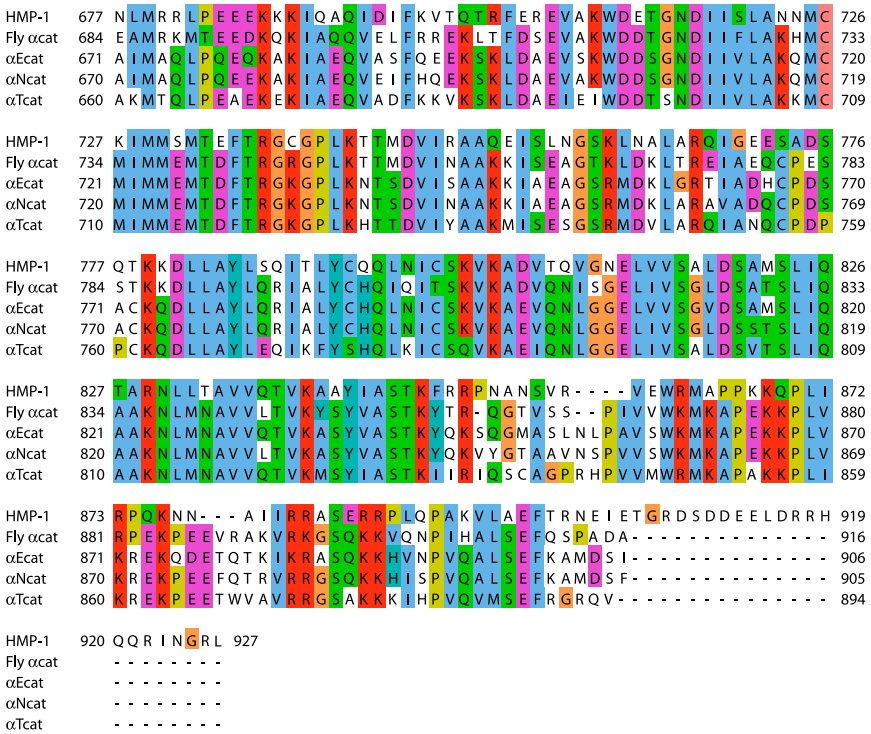

Fig. S3. Alignment of HMP-1, fly α-catenin, αE-catenin, αN-catenin and αT-catenin C-termini. Note the additional 23 aa C-terminal tail on HMP-1.